

Research Article

Characterization and *In Vitro* bioactivity of hydroxyapatite extracted from chicken bones for biomedical applications

Doaa Abbood CHALLOOB, Ali Taha SALEH*

Department of Chemistry, College of Science, University of Misan, Misan, Iraq.

*Email: alitaldosari@uomisan.edu.iq

Abstract: Due to low production costs and safety concerns, chicken bones have been the most common alternative source of Hydroxyapatite (HA). This study aimed to investigate the characterization and *in vitro* bioactivity of hydroxyapatite extracted biological HA from the chicken bone. The bones were washed and boiled in hot water before being calcined for two hours at 200, 400, 600, 800, 900, and 1000°C. The extracted powders were studied using X-ray diffraction (XRD), Fourier transforms infrared (FTIR), and field emission electron microscopy (FESEM). The results showed that the HA phase forms crystals when the chicken bones are heated to 900°C. The crystallinity and crystallite size significantly increased with increasing the heating treatment. The main functional hydroxyl and phosphate groups were found in the HA structure. The shape of extracted HA particles was globular. *In vitro* dissolution and bioactivity of biological HA were evaluated using simulated body fluid (SBF) for 1, 3, 7, and 14 days at 37°C. After the first day in SBF, the rate of deterioration was at its highest. It then went down gradually. The thickness of the apatite layer was significantly increased with a prolonged incubation period. There is hope that biological HA may be useful in the biomedical field.

Keywords: Chicken bone, Hydroxyapatite, Characterizations, Bioactivity.

Citation: Challob, D.A. & Saleh, A.T. 2023. Characterization and *In Vitro* bioactivity of hydroxyapatite extracted from chicken bones for biomedical applications. Iranian Journal of Ichthyology (Special Issue 1): 125-131.

Introduction

Reconstruction of a bone defect due to chronic disease or injury remains a challenge for clinicians. To repair a bone defect above a critical size, the use of synthetic biomaterial is usually required. Due to the limited supply of autologous bone and the threat of possible infection when using an allograft, it is necessary to use a synthetic biomaterial or xenograft, a bone segment from different animal species. The advantage of using xenogeneic bone is due to its similar structure and morphology to human bone (Akram et al. 2014; Wiweko et al. 2022). Grafts such as beef, mutton, pork, or fish bones contain trace ions which are readily available in large quantities and inexpensive to process. Inhomogeneous materials are first decomposed and then calcined at high temperatures (Pu'ad et al. 2019; Wiweko et al. 2022). The baking process is done to completely remove

organic components and destroy pathogens. The remaining ash contains bone mineral content. This HA extract contains valuable micronutrients that are known to play an important role in bone regeneration and promote the bone formation process (Pu'ad et al. 2019).

The incorporation of one or more trace ions into synthetic HA is a complex process that makes ion-substituted HA several times more expensive than regular HA (Panda et al. 2014). Hydroxyapatite can be synthesized from inorganic compounds or natural organic-based materials. In general, HA synthesized from natural organic sources is not stoichiometric, which may be due to the presence of trace amounts of natural anions biological resources (Mustafa et al. 2015). Although both types of biomaterials are inherently bioactive and biocompatible and considered equally suitable for *in vitro* use, the main

problem with biomaterials synthesized from inorganic sources of calcium and phosphorus is the high cost associated with the synthetic process.

Most traditional chemical methods are Na^+ , Zn^{2+} , Mg^{2+} , K^+ , Si^{2+} , Ba^{2+} , F^- , CO_3^{2-} etc. Contains HA synthesis without traces of useful elements. The presence of these ions directly affects various biochemical reactions associated with bone metabolism (Piccirillo et al. 2015). Useful cations such as hydroxyapatites produced from natural bone ash, eggshell or shell, Na^+ , K^+ , Mg^{2+} , Sr^{2+} , Zn^{2+} and Al^{3+} , or d-anions such as F^- , Cl^- , SO_4 and CO_3^{2-} or used in the presence of both has proven better for various medical applications, in particular for rapid bone regeneration (Granito et al. 2018). Synthetic pathways and methods to obtain CaP-based biomimetic ceramics and composites seem to be a good plan to further advance the synthesis of bioceramics with better properties (Neelakandeswari et al. 2011). Complete chemical formulations and composites combine the properties of calcium phosphates such as biocompatibility, non-toxicity, chemical and structural similarity to hard tissues with those of biocompatible or inert elements, increasing their bioactivity, mechanical strength, elasticity, their hierarchical structure and their porosity (Sofronia et al. 2014). This material has excellent bioactivity, high biocompatibility, and excellent osteoconductive characteristics (Ruksudjarit et al. 2008). Hydroxyapatite, HAp ($\text{Ca}_{10}(\text{PO}_4)_6(\text{OH})_2$), is thermodynamically stable in crystalline body fluid and has a very similar composition to bone mineral (Jaber et al. 2018). HAp can integrate with bone without causing any local or systemic toxicity, inflammation or foreign body response (Kerian 2019). For these reasons, HAp is mainly used in biomedical applications and not as a veneering material for orthopedics, dentistry, and metal implants (Mondal et al. 2012). Therefore, HAp synthesis methods with customizable properties have been widely studied. Synthetic HAp can be produced by a variety of methods, including dry (solid state and mechanochemical) methods (Khoo et al. 2015), wet

methods (chemical precipitation, hydrolysis, sol-gel, hydrothermal, emulsion and sonochemical) and high-temperature processes (combustion and pyrolysis) (Ojo et al. 2022). Compared to synthetic HAp, natural HAp is non-stoichiometric since it contains trace elements such as Na^+ , Zn^{2+} , Mg^{2+} , K^+ , Si^{2+} , Ba^{2+} , F^- , and CO_3^{2-} which make it similar to the chemical composition of human bone (Lertcumfu et al. 2016). Based on the above-mentioned background, this study aimed to investigate the characterization and *in vitro* bioactivity of hydroxyapatite extracted biological HA from the chicken bone.

Materials and Methods

The chicken bones were purchased from the local market in Misan, Iraq. The bones were cut up using a sharp knife and brought together once they had been collected. The pieces were cooked for about four hours in a sealed container to remove any big impurities that had adhered to them. The samples were then washed several times with distilled water before being submerged in a 3:1 mixture of acetone and ether for three hours to remove unseen fat and finally dried in a hot air oven at 120°C for 17 hours to prevent the development of shoots during the grinding process. The raw powder was then put through the calcination process, which consisted of it being heated in a furnace at temperatures ranging from 200 to 1000°C at a pace of 5°C per minute for a total of 2 h. The results showed that the chicken bones treated to temperatures ranging from 200 to 800°C have a black or light gray color (Fig. 1). This indicates that the material is amorphous and highly carbonated by the residues of the organic materials. By heating the chicken bone powders between 900 and 1000°C , the color changes from light gray to pure white milky (Fig. 1). This demonstrates that organic materials are removed, and pure HA particles are crystallized. As a direct result of this, it was shown that the ideal temperature range for forming the HA phase was between 900 and 1000°C . Using different methods, the white powder was studied to investigate



Fig.1. Shows the collected bones treated at different temperatures.

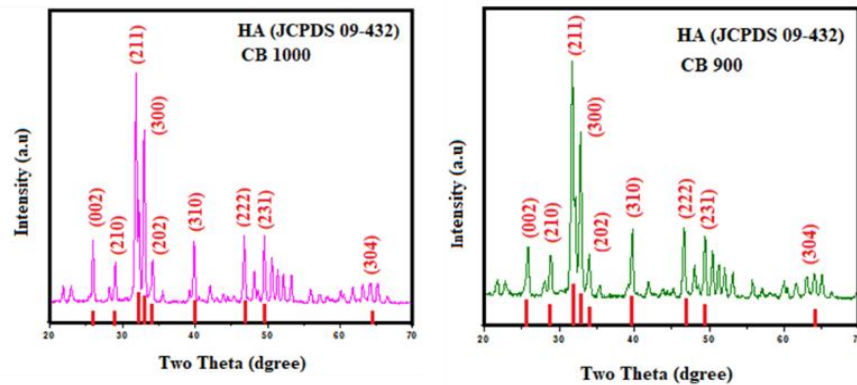


Fig.2. XRD pattern of HA calcined at (a) CB 900) and (b) CB1000°C for 2h.

its microstructure. The phase purity, lattice parameters, crystallite size, and degree of crystallinity were investigated using X-ray diffraction (XRD, Philips1730, PANalytical B.V.). The functional groups such as hydroxyl, carbonate, and phosphate groups that existed in the obtained powders were investigated using Fourier-transform infrared spectroscopy (FTIR, Nicolet iS50 spectrometer). To determine particle size and shape, field emission scanning electron microscopy (FESEM, Oxford Instruments Swift ED 3000) was used. A very thin layer of gold was applied to the samples beforehand to reduce the amount of sparks produced. A model of the simulated body fluid (SBF) was used to assess the degradation and bioactivity of the extracted HA. The specimens, which were in the shape of discs, were put inside

polyethylene vials that contained 50mL of SBF, and then the vials were covered with a lid. They were shaken in a water bath for 1, 3, 7, and 14 days while incubating at 37°C. At each interval, the discs were meticulously removed from the SBF, rinsed in ethanol and distilled water, and then air-dried at room temperature. The next phase consisted of doing a FESEM-EDX examination to investigate the apatite layer that had formed on their surface and establish the Ca/P ratios. A tiny sample of each supernatant was collected at each time point, and the amount of Ca^{2+} ions released was measured using Flame atomic absorption spectroscopy (Al 1200, Aurora, UK).

Results and Discussion

A phase investigation of the HA was carried out using XRD (Fig. 2). Crystallization of HA occurs

Table 1. Lattice parameters, degree of crystallinity and crystallite size of biological HA f at 900°C and 1000°C.

Sample ID	Lattice Parameters			X_c (%)	CS (nm)
	a (Å)	c (Å)	V (Å) ³		
Standard HA	9.418	6.884	528.8	-	-
FB-900 °C	9.416	6.863	527.3	87.77	30.04
FB-1000 °C	9.417	6.860	527.1	79.31	53.79

• X_c = degree of crystallinity; CS = crystallite size.

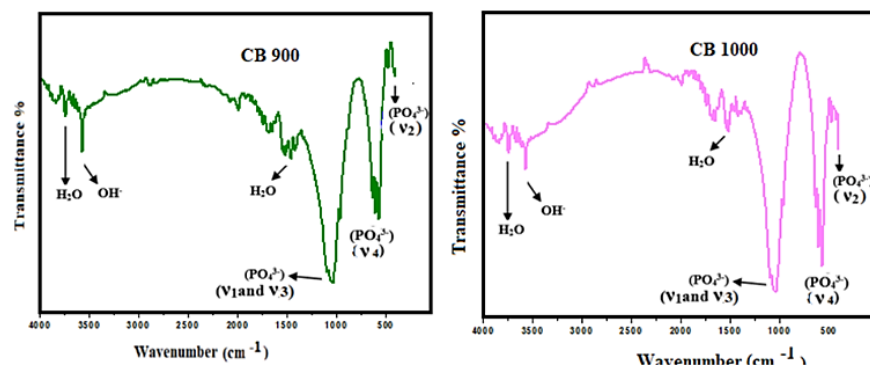


Fig.3. FTIR Spectra of HAp powder Calcined at (a) CB 900) and (b) CB1000°C for 2h.

successfully after calcination at temperatures between 900 and 1000°C. The peaks in the XRD pattern for HA were found to be located at the coordinates 26.12°, 28.45°, 31.15°, 33.20°, 34.28°, 40.11°, 46°, (49.47°, and 55°). These peaks correspond to the 002, 210, 211, 300, 202, 310, 222, 213, and 304 planes of crystalline HA. It has been determined that HA crystallizes in a hexagonal structure with the following lattice parameters: $a = b = 9.416\text{Å}$, $c = 6.863\text{Å}$, and cell volume = 527.3Å^3 . The diffraction peaks and lattice parameters were in good agreement with the standard phase of HA (JCDPS 09-432). Along with the main peaks of HA, a tiny peak at 30.71° was observed with an increase in the calcination degree to 1000°C, which could be attributed to the 0210 diffraction plane of β -tricalcium phosphate (β -TCP, JCDPS No. 09-0169). The β -TCP phase appears as a minor phase as a result of HA decomposition at high temperatures (Nilen & Richter 2008). Furthermore, no significant changes were observed in terms of lattice parameters, degree of crystallinity, or crystallite size (Table 1).

The presence of the functional groups in the extracted HA was detected using FTIR analysis, and the results are shown in Figure 3. Four vibrational modes of the phosphate (PO_4^{3-}) group were recorded

at 466cm^{-1} (PO_4^{3-} (v4), 565cm^{-1} (PO_4^{3-} (v2), 604cm^{-1} (PO_4^{3-} (v2), and $921\text{-}1200\text{cm}^{-1}$ (PO_4^{3-} (v1,3). The stretching and bending modes of the hydroxyl (OH) group were observed at 3566cm^{-1} and 634cm^{-1} , respectively. Furthermore, the vibrational modes of carbonate (CO_3^{2-}) were detected at 1406cm^{-1} and 1514cm^{-1} . The presence of carbonate groups is an indication of the formation of carbonated HA. Nonetheless, it is possible that the presence of CO_3^{2-} really enhances the bioactivity of HA, thus it should not be observed as a negative thing. The sharpness of the phosphate and hydroxyl bands showed the formation of crystalline HA. Increasing calcination temperatures to 1000°C increased the sharpness of the PO_4^{3-} (v1,3) group, which could be attributed to a higher degree of crystallinity (Table 1). While the intensity of the OH group's stretching mode decreased with increasing calcination degree, this behavior could be attributed to the decomposition of HA to β -TCP.

FESEM micrographs of calcined extracted powders at 900 and 1000°C showed the particles to be irregularly formed agglomerates that were densely packed together (Fig. 4). During the creation of HA particles, one or more of the following steps may occur: a) the production of HA via the processes of

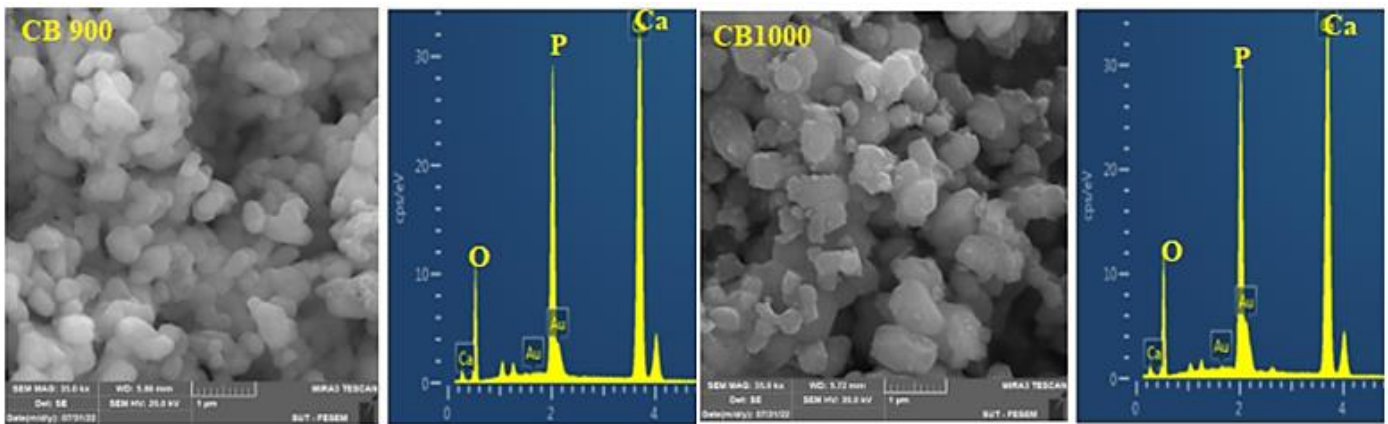


Fig.4. FESEM images of CB-900°C and CB-1000°C.

Table 2. Release of Ca^{2+} ion in SBF over 14 days at 37°C.

Immersion time (day)	Release of Ca^{2+} ion (mg/L) in SBF	
	HA (CB 900)	HA(CB 1000)
0.0	13.12	12.90
1	23.87	22.88
3	14.79	15.10
7	11.55	10.13
14	9.95	10.07

- STDEV \pm 0.32-0.72

nucleation and growth surface free energy is reduced as a consequence of (b) the aggregation of elemental crystals via the molecular attractions of unique scale forces. This causes a decrease in surface free energy. The production of additional crystals inside the aggregates, which occurs under a continuous residual supersaturation, leads to aggregation. After then, this agglomerated particle joins forces with other particles to form secondary particles, which subsequently increase in size.

The results of an *in vitro* dissolution evaluation using SBF that lasted for 14 days and was conducted to determine the dissolution behavior of FB-900°C are shown in Table 2. The results provide insight into the possible Ca^{2+} ion concentration present in SBF throughout the course of a period of 14 days. The results demonstrate that the release of Ca^{2+} ions happened quite fast, which signaled the beginning of the pellet's dissolution on its most superficial layers. Ca^{2+} ions concentrations reached their zenith after 24 hours after immersing in SBF, when they were at their maximum. During the first 24 hours after SBF

immersion, the deposition process, on the other hand, emerged as the most important step. The consumption of Ca^{2+} ions may explain the drop in the concentration of Ca^{2+} ions observed during the development of the apatite layer. Maintaining a constant level of Ca^{2+} concentrations over a period of 7-14 days is evidence that a balance has been struck between the processes of deposition and dissolution.

After just one day in the SBF, the surface of each sample exhibited evidence of apatite particle development (Fig. 5). After a period of one day, increased apatite particle growth was observed. This was attributed to a reduction in sample crystallinity, which made it possible to significantly and quickly release Ca^{2+} ions. After 7 and 14 days in the immersion medium, homogeneous development was observed. The length of time that the sediment was submerged resulted in an increase in the apatite layer's thickness that had just been produced.

The EDX analysis revealed that the majority of the formed surface particles were composed of calcium, phosphorus, and oxygen, with the, Ca and P content

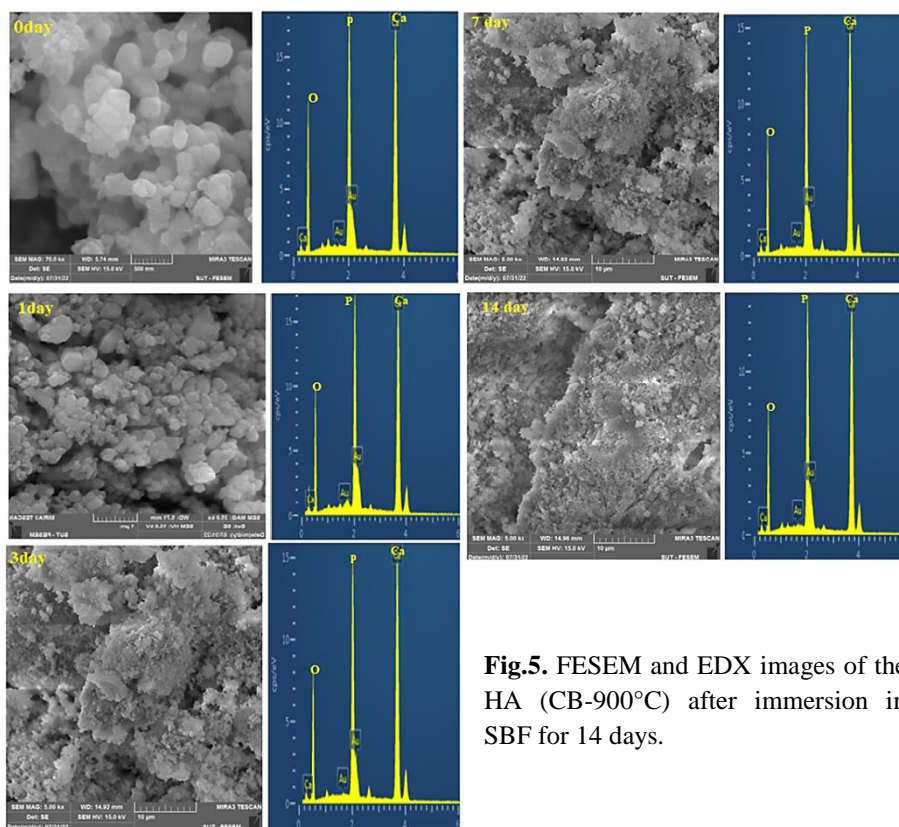


Fig.5. FESEM and EDX images of the HA (CB-900°C) after immersion in SBF for 14 days.

steadily decreasing as the immersion period increased. This occurred due to the transformation of the Ca rich-ACP that was initially generated into a layer of stoichiometric crystalline apatite.

References

- Akram, M.; Ahmed, R.; Shakir, I.; Ibrahim, W.A.W. & Hussain, R. 2014. Extracting hydroxyapatite and its precursors from natural resources. *Journal of Materials Science* 49: 1461-1475.
- Granito, R.N.; Renno, A.C.M.; Yamamura, H.; de Almeida, M.C.; Ruiz, P.L.M. & Ribeiro, D.A. 2018. Hydroxyapatite from fish for bone tissue engineering: A promising approach. *International Journal of Molecular and Cellular Medicine* 7(2): 80.
- Jaber, H.L.; Hammood, A.S. & Parvin, N. 2018. Synthesis and characterization of hydroxyapatite powder from natural camelus bone. *Journal of the Australian Ceramic Society* 54(1): 1-10.
- Kerian, K. 2019. Synthesis and characterization of hydroxyapatite powder from fish bones and scales using calcination method. *Synthesis* 28(18): 82-87.
- Khoo, W.; Nor, F.M.; Ardhyantana, H. & Kurniawan, D. 2015. Preparation of natural hydroxyapatite from bovine femur bones using calcination at various temperatures. *Procedia Manufacturing* 2: 196-201.
- Lertcumfu, N.; Jaita, P.; Manotham, S.; Jarupoom, P.; Eitssayeam, S.; Pengpat, K. & Rujijanagul, G. 2016. Properties of calcium phosphates ceramic composites derived from natural materials. *Ceramics International* 42(9): 10638-10644.
- Mondal, S.; Mondal, B.; Dey, A. & Mukhopadhyay, S.S. 2012. Studies on processing and characterization of hydroxyapatite biomaterials from different bio wastes. *Journal of Minerals and Materials Characterization and Engineering* 11(1): 55-67.
- Mustafa, N.; Ibrahim, M.H.I.; Asmawi, R. & Amin, A.M. 2015. Hydroxyapatite extracted from waste fish bones and scales via calcination method. In *Applied mechanics and materials* (Vol. 773, pp. 287-290). Trans Tech Publications Ltd.
- Neelakandeswari, N.; Sangami, G. & Dharmaraj, N. 2011. Preparation and characterization of nanostructured hydroxyapatite using a biomaterial. *Synthesis and Reactivity in Inorganic, Metal-Organic, and Nano-Metal Chemistry* 41(5): 513-516.
- Nilen, R.W.N. & Richter, P.W. 2008. The thermal stability of hydroxyapatite in biphasic calcium phosphate ceramics. *Journal of Materials Science:*

Materials in Medicine 19: 1693-1702.

- Ojo, O.E.; Sekunowo, O.I.; Ilomuanya, M.O.; Gbenebor, O.P. & Adeosun, S.O. 2022. Structural and morphological evaluations of natural hydroxyapatite from calcined animal bones for biomedical applications. *Journal of Casting and Materials Engineering* 6(1): 2.
- Panda, N.N.; Pramanik, K. & Sukla, L.B. 2014. Extraction and characterization of biocompatible hydroxyapatite from fresh water fish scales for tissue engineering scaffold. *Bioprocess and Biosystems Engineering* 37(3): 433-440.
- Piccirillo, C.; Pullar, R.C.; Costa, E.; Santos-Silva, A.; Pintado, M.M.E. & Castro, P.M. 2015. Hydroxyapatite-based materials of marine origin: A bioactivity and sintering study. *Materials Science and Engineering C* 51: 309-315.
- Pu'ad, N.M.; Koshy, P.; Abdullah, H.Z.; Idris, M.I. & Lee, T.C. 2019. Syntheses of hydroxyapatite from natural sources. *Heliyon* 5(5): e01588.
- Ruksudjarit, A.; Pengpat, K.; Rujijanagul, G. & Tunkasiri, T. 2008. Synthesis and characterization of nanocrystalline hydroxyapatite from natural bovine bone. *Current Applied Physics* 8(3-4): 270-272.
- Sofronia, A.M.; Baies, R.; Anghel, E.M.; Marinescu, C.A. & Tanasescu, S. 2014. Thermal and structural characterization of synthetic and natural nanocrystalline hydroxyapatite. *Materials Science and Engineering C* 43: 153-163.
- Wiweko, A.; Yudhanto, D.; Rizki, M.; Habib, P.; Dirja, B.T. & Rosyidi, R.M. 2022. Treatment of bone defects with bovine hydroxyapatite xenograft and platelet rich fibrin (PRF) to accelerate bone healing. *International Journal of Surgery Case Reports* 97: 107370.